Polymer Testing 90 (2020) 106729

Contents lists available at ScienceDirect

Polymer Testing

journal homepage: http://www.elsevier.com/locate/polytest

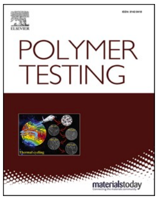

Material Properties

Industrially produced PET nanocomposites with enhaced properties for food packaging applications

T. Fernández-Menéndez [a], D. García-López [b], A. Argüelles [c], A. Fernández [d], J. Viña [a,*]

[a] Department of Materials Science and Metallurgical Engineering, Campus Universitario, 33203, Gijón, Asturias, Spain
[b] SMRC Automotive Interiors Spain S.L.U., Pol. Ind. Alto de San Juan, C/ Radilla, sn, 47800, Medina de Rioseco, Valladolid, Spain
[c] Department of Construction and Manufacturing Engineering, Campus Universitario, 33203, Gijón, Asturias, Spain
[d] Klöckner Pentaplast, 33128, Vegafriosa s/n, Asturias, Spain

ARTICLE INFO

Keywords:
Poly (ethylene therephthalate)
PET
Sepiolite
Clay
Nanocomposite
Extrusion
Thermoforming

ABSTRACT

Gas permeation of polymers is one of the important factors to be considered in the selection of materials for many packaging applications, such as modified atmosphere packaging (MAP) for foods. Poly (ethylene therephthalate) (PET) is known to exhibit very low gas permeation compared with most polymers such as polystyrene, polyethylene and polypropylene. However, MAP applications require better barrier performance than that of PET. In the present work PET trays reinforced with organically modified sepiolite, fibrillar nanoclay, have been produced at industrial processes. Permeability to water vapour, oxygen and carbon dioxide has been studied in PET nanocomposites as well as their microstructure through transmission electron and scanning electronic microscopy (TEM and SEM), and their mechanical properties. Results show a better performance in barrier properties as well as an increase in tensile strength, and impact resistance when the sepiolite content is lower than 2.5%.

1. Introduction

Nanotechnology has brought the opportunity of improving polymer properties for basically all technical disciplines; such as polymeric nanobiomaterials [1–4] and nanobiomedicine [5], nanoelectronics [6,7] or nanocomposites [8–12]. Between these nanocomposites, one of the most widely studied has been layered clay/polymer nanocomposites [13–17], being montmorillonite (MMT) the most studied clay in this field [18,19]. However, there are other clays worth studying for their application in nanotechnology, such as sepiolite. Sepiolite is a hydrated magnesium silicate mineral, with chemical formula $Mg_4Si_6O_{15}(OH)_2{\cdot}6H_20$ [20,21] and microfibrous morphology [22,23] with high aspect ratio and two dimensions in the nanometer scale [24], thus, a nanofiber according to EFSA definitions. What makes this clay very attractive to industry are its surface properties [25]; due to its structure, sepiolite has silanol groups (Si–OH) on its external surface, which allow for the preparation of organic-inorganic materials [26].

And this study will review the use of nanosepiolite clay as a reinforcement in PET matrix nanocomposites for their use in industrial food packaging applications.

Poly (ethylene therephthalate), PET, has some characteristics that make it very useful for food packaging, such as transparency, chemical resistance, medium barrier to gases, good recyclability and mechanical properties. Therefore, it is one of the most widely used polymers for food packaging. However, packaging must be under continue development due to consumer demand in achieving higher durability while keeping product freshness characteristics. As a response to these requirements modified atmosphere packaging (MAP) has developed [27–29]. Modified atmosphere packaging requires the elimination of the air within the package and then, as a function of the technology used, a gas or a mix of gases may be injected, depending on the food type. For these packaging, polymers with good barrier properties to gases are used, that is to say, polymers with low permeability to gases. Although PET has acceptable gas barrier properties for many applications, it requires improvement for modified atmosphere packaging, when long shelf life is required. For these applications, multilayer sheets such as polymer/barrier-film/sealable-film including ethylene vinyl alcohol copolymer (EVOH) are generally used. Industrially the use of multilayer sheets implies an increase in complexity within the production process. It requires the incorporation of a new process, such as lamination or coextrusion, while the recyclability of the final tray highly decreases. Besides, with the use of nanoparticles, mechanical, thermal and barrier properties can be improved [8,30,31]. Thus, it is very interesting to work on the development of new PET nanocomposites with enhanced barrier properties [32–42] at an industrial stage.

---

* Corresponding author.
E-mail address: jaure@uniovi.es (J. Viña).

https://doi.org/10.1016/j.polymertesting.2020.106729
Received 11 May 2020; Received in revised form 26 June 2020; Accepted 2 July 2020

Nomenclature

MAP	Modified Atmosphere Packaging
PET	Poly(ethylene terephthalate)
SEM	Scanning Electron Microscopy
TEM	Transmission Electron Microscopy
MMT	Montmorillonite
EVOH	Ethylene Vinyl Alcohol Copolymer
MEMO	γ-methacryloxypropyltrimethoxy
TGA	Thermogravimetric Analysis
RH	Relative Humidity
nS	Nano-Sepiolite
PC	Permeability Coefficient
EFSA	European Food Safety Approval

2. Experimental part

2.1. Materials

PET pellets are form Novapet S.A., and were kindly supplied by LINPAC Packaging Pravia S.A.U. (Asturias, Spain) as well as PET-EVOH-PE laminated sheet. These PET pellets are specially conceived for film packaging and sheeting applications via extrusion, being its viscosity of 0.79 dL/g. The sepiolite (Pangel S9), modified with γ-methacryloxypropyltrimethoxy (MEMO) silane (approved, by Regulation CE 975/2009, for food contact applications), was kindly supplied by TOLSA S.A. (Madrid, Spain) in the form of fine powder, and Repol S.A. (Castellón, Spain) produced the PET/nanosepiolite master by melt-blending in an extrusion pelletizing machine.

2.2. Nanocomposites sheet production and tray production

Processing conditions, such as type of extrusion (mono screw or twin screw), extrusion speed (rpm and discharge pressure controlled) and melt temperature, have a huge influence in nanocomposites morphology and viscosity, and thus in nanocomposites properties. Two masters with different nanosepiolite concentrations (8.77% and 16.3%) were prepared by melt blending at Repol in an industrial polyamide low shear extruder. These masters were used to produce nanocomposite sheets in an industrial co-rotating twin screw extruder (LINPAC Packaging Pravia) at 736–1246 kg/h and 270 °C, with final nanosepiolite concentrations ranging from 1 to 3%. The extrusion speed was kept high, at 1246 kg/h, since at low values the discharge pressure highly decreases, which indicates a lower residence time is best for the nanocomposites viscosity and hence, their mechanical properties. The trays were produced in a Kiefel thermoformer.

2.3. Nanocomposites characterization

2.3.1. Thermal analysis

Thermogravimetric Analysis (TGA) was used to determine nanosepiolite percentage within the nanocomposite sheets. The analyses were performed in a Mettler Toledo 851e equipment, using a procedure in two steps:

1st step: from 50 °C to 600 °C at 20 °C/min under nitrogen atmosphere.

2nd step: from 600 °C to 900 °C at 20 °C/min under air atmosphere.

2.3.2. Microscopic characterisation

Scanning Electron Microscopy (SEM) was performed on a fractured surface after a treatment in liquid nitrogen using a Hitachi 3400 N microscope.

Transmission Electron Microscopy (TEM) was used to analyse the nanosepiolite nanometric dispersion/defibrillation in the nanocomposite's sheets. Sample preparation was made with an ultramicrotome in liquid nitrogen. The TEM microscope used was a JEOL 200FX at 200 kV.

2.3.3. Barrier properties

The permeability analyses were done on sheet samples; specimens taken from the extruded sheets before going to thermoforming into trays.

Water vapour transmission rate was measured with a Permatran W398, from "Modern Control, Inc" (MOCON). The tests were carried out according to the Standard ASTM E398 [43], being the test conditions 38 °C, 90% relative humidity and 760 mmHg.

Oxygen transmission rate was measured in an OXTRAN with a volumetric sensor (MOCON, Oxtran SS 2/20). Previously to the analysis the samples were upgraded, 48 h under an atmosphere with 0% RH. Oxygen transmission rate was measured at 23 °C and 0% RH following Standard ASTM D3985 [44].

Carbon dioxide transmission rate was measured in a Permatran C-200 (MOCON), with an infrared sensor. Specimens were previously upgraded under at atmosphere with 0% RH for 48 h. The transmission rate determination was done at 23 °C and 0% RH following the Standard ASTM D3985. For all the transmission rate tests, the effective area exposed to permeation was 50 cm^2.

2.3.4. Mechanical properties

The mechanical properties were evaluated both in the extruded sheet and on the final thermoformed tray. Tensile testing on sheet was carried out on an Instron Model 5582 (100 kN) equipped with a load cell of 5 kN according to Standard ISO 527-3 on type 5 specimens and a crosshead speed of 100 mm/min. The samples were cut in longitudinal direction from the extruded sheet.

The tray chosen has been a MAP tray with the following measures: 18 cm length, 25 cm width and 25 cm depth (see Fig. 1). Impact strength on trays was carried out on an Izod pendulum from TMI (Monitor/Impact Testing Machines Inc.) using weight of 5 pounds. Tests were done under internal procedure specially developed for trays, although based on ISO:180–2001 [45]. In this procedure, the trays are anchored to the equipment with the pendulum hitting tray's side walls and seal edges (Fig. 2a and 2b).

Lateral compression test and stiffness were tested on a Hounsfield H1KS Benchtop equipment (Fig. 3) following internal procedures for trays.

Fig. 1. Reference tray by courtesy of LINPAC Packaging Pravia.

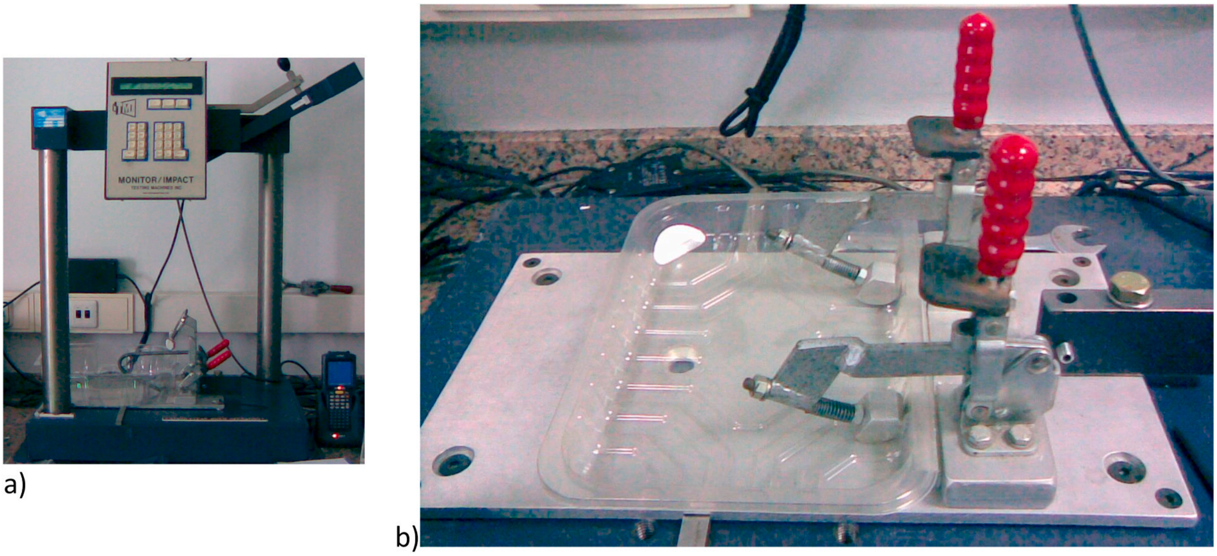

Fig. 2. a) Impact testing machine. b) Specific anchorage for these trays.

Fig. 3. Hounsfield equipment for compression and stiffness tests on trays.

3. Results and discussion

3.1. Thermal analysis

Table 1 shows the percentage of sepiolite in the master and Table 2 shows the final percentage of sepiolite on the extruded sheet. The percentages of sepiolite shown in the tables below are the final amounts of clay both in the masters and in the sheets, once PET residue has been discounted from the results in the thermograms.

Samples from M0 to M5 were obtained from master 1, while M6 and M7 come from master 2. This was due to a limitation in the extruder dosing system for additives.

3.2. Microscopic characterisation

The morphology of the fracture surface of PET/nanosepiolite composite is shown in Fig. 4. All the SEM samples were analysed in the longitudinal way, following the extrusion direction, in order to observe the length and the defibrillation of the nanosepiolite within the PET matrix.

The SEM examination shows differences regarding morphology and dispersion depending on the nanosepiolite master and the final concentration of the clay within the matrix. In Fig. 4a) nanosepiolite particles are not seen, probably due to a good dispersion of the clays within the PET matrix. This sample, M1, was obtained from a master with 8.77% of nanosepiolite, and TGA tests revealed a nanosepiolite concentration of 1.2%. In samples with higher concentration of sepiolite, SEM micrographs reveal micrometric organo-sepiolite aggregates within the PET matrix. Fig. 4b) and 4c) show two nanocomposite samples with 2.73% and 3.02% of organo-sepiolite obtained from two different masters, with 8.77% and 16.30% of nanosepiolite respectively. The organo-modifier in all these samples is the silane MEMO.

The sample M7, with 3.02% of sepiolite, shows a higher number of micrometric aggregates, with sizes between 0.5 and 1 μm.

With the aim of verifying the nanometric dispersion of the nanosepiolite within the nanocomposite TEM analysis of the samples was done. Fig. 5 shows TEM images that are representative of the

Table 1
Residue content in the master.

	Master 1	Master 2
Average TGA residue (%)	8.77 ± 0.3	16.30 ± 1.2

Table 2
Residue content in pure PET and sepiolite nanocomposites.

	Pure PET	Nanocomposite sheet							
		M0	M1	M2	M3	M4	M5	M6	M7
Average TGA residue (%)	0.42	0.9	1.20	1.31	1.8	2.1	2.2	2.73	3.02

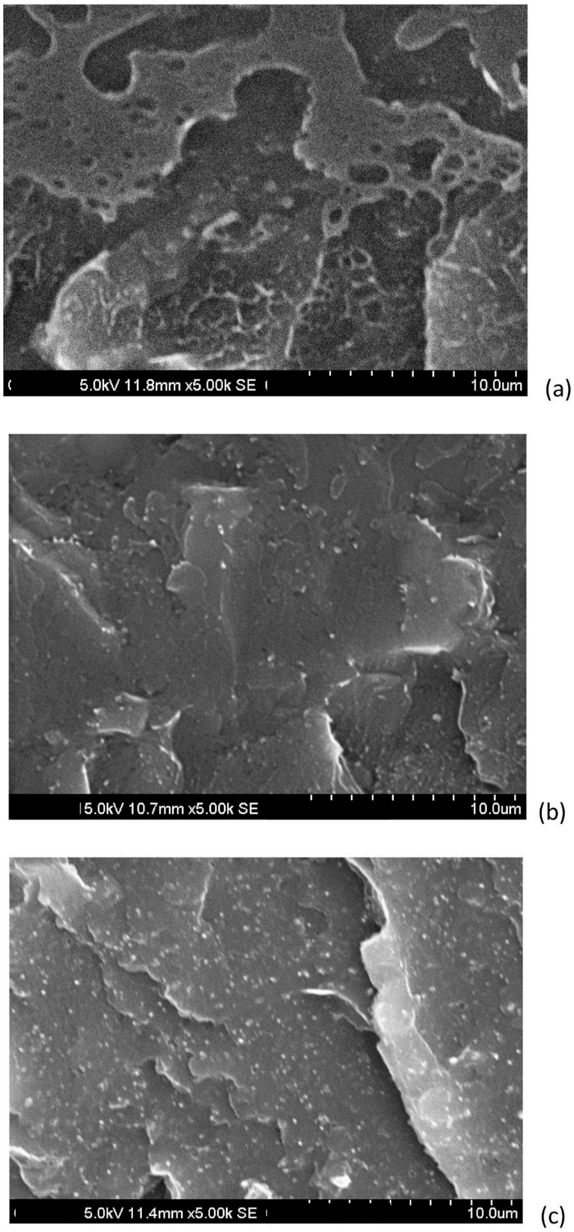

Fig. 4. SEM pictures taken from samples fractured in liquid nitrogen a) sample with 1.2% nanosepiolite from master 8.77% (M1); b) sample with 2.73% nanosepiolite from master 16.30% (M6); c) sample with 3.02% nanosepiolite from master 16.30% (M7).

nanocomposite's morphology. These images show a heterogeneous morphology without preferred orientation in extrusion direction, with individual nanofibers (rectangles) together with nanofiber aggregates (blue arrows) randomly dispersed in the PET matrix. It is also observed that some nanofibers are more than 500 nm length, although most of them are shorter and some even broken nanofibers (ellipses). The presence of these broken fibres could be due to the nanocomposites sheet fabrication process (two extrusion steps). The composite exhibits fibrous morphology and some sepiolite aggregated fibres.

On the other hand, analyzing the same sample but after a transversal cut, it can be seen a good dispersion of nanosepiolite within the matrix, and that both nanofibers and clusters appear broken do to sample cut orientation (Fig. 6).

Looking at Fig. 6, it seems that the morphology of the nanocomposites is quite similar in all the samples. However, in Fig. 7, it can be seen that the samples with lower content of nanosepiolite (Fig. 7a) presents a better dispersion/defibrillation of the nanofibers, presenting longer nanosepiolite fibres and less aggregates than Fig. 7b, with higher amount of nanoclay.

The SEM and TEM results indicate that the sepiolite fibres are completely disordered and dispersed relatively homogeneous into the PET matrix. This could mean that the big silane molecules (MEMO) are doing their job, interacting between the sepiolite and the polar groups in the PET matrix.

3.3. Permeability properties

The permeability properties have been analysed for oxygen, water vapour and carbon dioxide as diffusing gases which influence food degradation, such as oxidation or microbial growth. In order to compare the permeability properties of the different sheet samples, it has been calculated the permeability coefficient (PC). PET-EVOH-PE sheet values are also shown because it is one of the most used polymers for food packaging under MAP conditions, requiring long shelf life.

From the results shown in Fig. 8, it can be seen that the permeability to O_2 and CO_2 improved in all the nanocomposite samples, compared to that of pure PET matrix. The improvements are of 8–24% for oxygen (Figure 8a), 8–35% for carbon dioxide (Fig. 8b). In case of H_2O the improvements start from 1% up until 10% over that of pure PET (Fig. 8c). It seems that the best barrier properties are for samples with more than 1% of nanoclay. For the sample with 0.9% nanosepiolite the improvement in O_2 and CO_2 permeability compared to that of PET is very little, and for water vapour there is no improvement. So, it can be stated that with less than 1% of nanoclay, there is not enough obstacle for gases and vapours molecules to go through. It is when the content of nanosepiolite is over 1% that it has been seen an improvement in PET barrier properties [46,47]. The best results are for the sample M6, which has 2.73% of nanosepiolite, followed very closely by results obtained in samples with 1.20% of nanoclay. This would indicate, that in that sample, a very well sepiolite dispersion has been achieved within the PET matrix. When increasing the amount of nanoclay in the polymer matrix (over 3%), the processability of the nanocomposites gets more difficult, due to a drop in the discharge pressure of the extruder, which means there is a decrease in the viscosity of the material. This could be due to the hygroscopic behaviour of the nanosepiolite, which incorporates water to the system, hydrolysing PET matrix. Besides, results show that increasing the nanosepiolite to 3% makes the dispersion worse and more clusters are formed (Fig. 7). This is the reason why no trials were done with nanosepiolite content over 3%. Similar results were obtained by Ke Z. and Yongping B [46]. where they found out that they could not produce PET film with organo-modified montmorillonite with more than 3% of organoclay content due to film-form properties. The permeability of the samples follows the tendency seen in previous works [47,48]; this is, permeability is reduced when increasing the nanosepiolite content. However, as seen in the results above, it is possible to decrease the amount of nanoclay in the samples, as long as

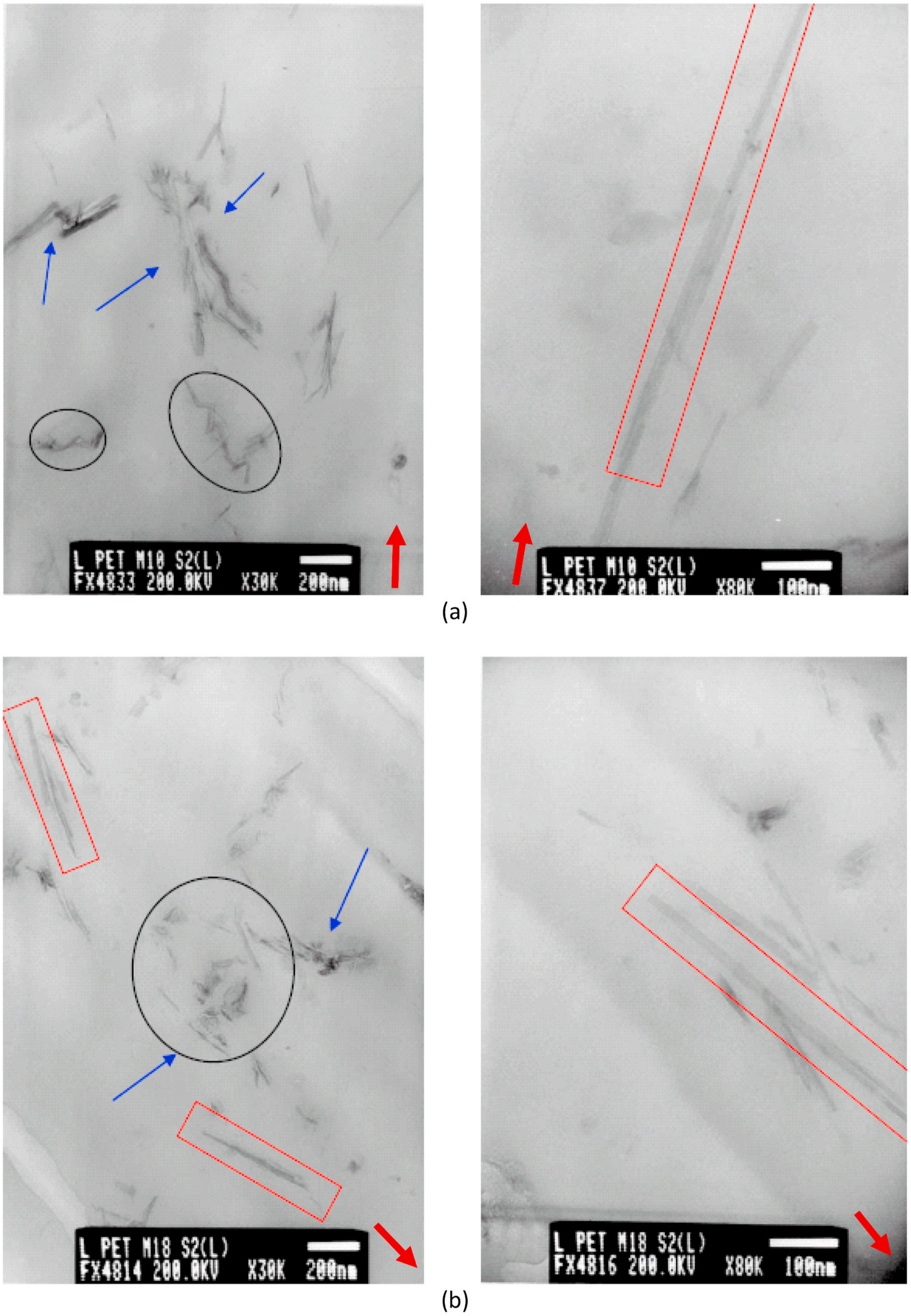

Fig. 5. TEM microstructure of PET/nanosepiolite composites, longitudinally cut. a) Sample with 1.2% nanosepiolite from master 8.77% (M1); b) sample with 2.73% nanosepiolite from master 16.30% (M6). Red arrows showing extrusion direction.

the nanoparticles are well dispersed and oriented within the matrix. Thus, the key points to achieve good barrier properties is to combine a certain amount of nanoclay, with a good dispersion and orientation [49–52]. If the sepiolite content is too low it will not do the job and if it is too much, PET matrix viscosity will decrease and it will not disperse properly, opening the path for gases and vapours molecules.

3.4. Mechanical properties of nanosepiolite sheets

Tensile strength and elongation at break tests, carried out according to ISO 527-3, with Type 5 specimens. Tensile strength of nanocomposite sheets increases up until 28% over that of pure PET for the sample with the highest content of sepiolite. This could be attributed to high stiffness of the clay, together with a good affinity between PET and the

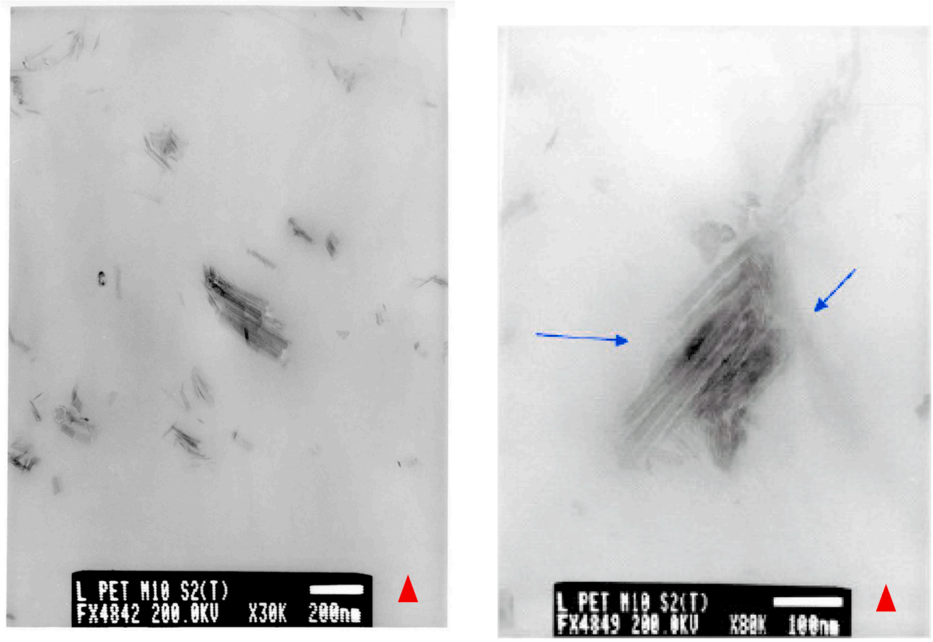

Fig. 6. TEM microstructure of sample M1, with 1.2% sepiolite transversally cut. Red arrows showing extrusion direction, in this case the arrow would go out of the paper, perpendicularly.

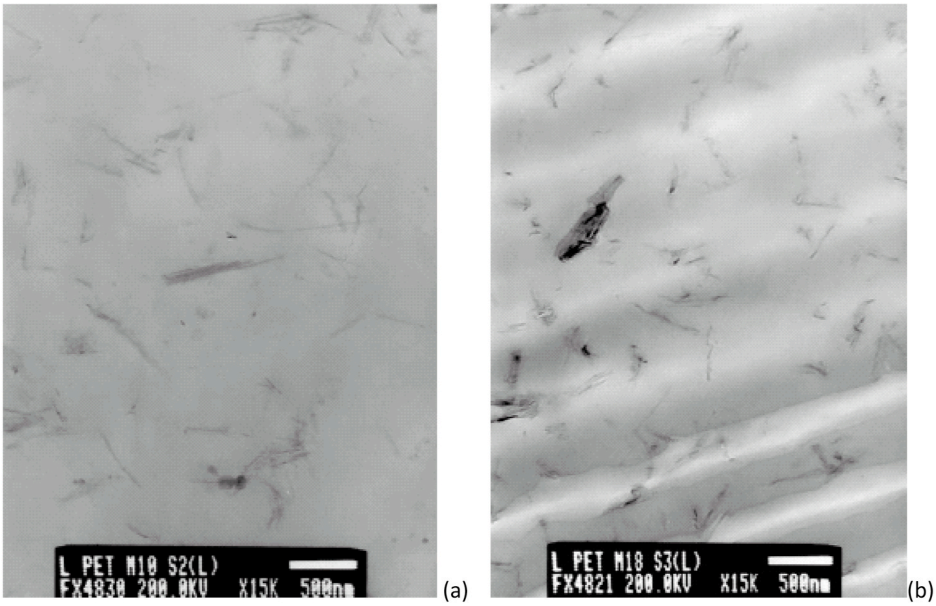

Fig. 7. TEM images of the PET/nanosepiolite composite with different nanoclay concentrations; a) 1.2% nanosepiolite, b) 3.02% nanosepiolite.

organosepiolite [53] and a relatively good clay dispersion [54]. This could be explained by the large specific area and active centres of the sepiolite, which means more physical and chemical interactions with the polymer matrix [55]. According to many clay/nanocomposite references, it is seen an increase in the tensile strength when increasing the amount of nanoclay in the sheet as Fig. 9 shows [53,56]. However, in this case, the increase is just of 4% comparing the sample with 0.9% to the 3%. This is probably due to a not completely well dispersed nanosepiolite, with clusters formation, and also to the PET matrix degradation observed for the 3% nanoclay sample.

Although elongation at break tests results showed a high degree of dispersion, it can be observed a decrease in the results when increasing the amount of sepiolite (Fig. 10). That variability in the results could be due to the sepiolite clusters, which generates points of brittleness in the nanocomposite sheet. Also, as seen in the TEM figures, the particles distribution within the nanocomposite is quite heterogeneous and without preferred orientation. This distribution could cause the coalescence of empty spaces generated around the nanoparticles when the material is under tensile loads, which would lead to a decrease in elongation at break [57].

Tensile strength and elongation at break results suggest a good interfacial adhesion between organo- modified sepiolite and the PET matrix. When a good interface exists between the nanoparticle and its matrix it is necessary to apply a higher tensile stress to break the material; at the same time elongation at break should decrease when increasing the interfacial adhesion but it also depends on the dispersion

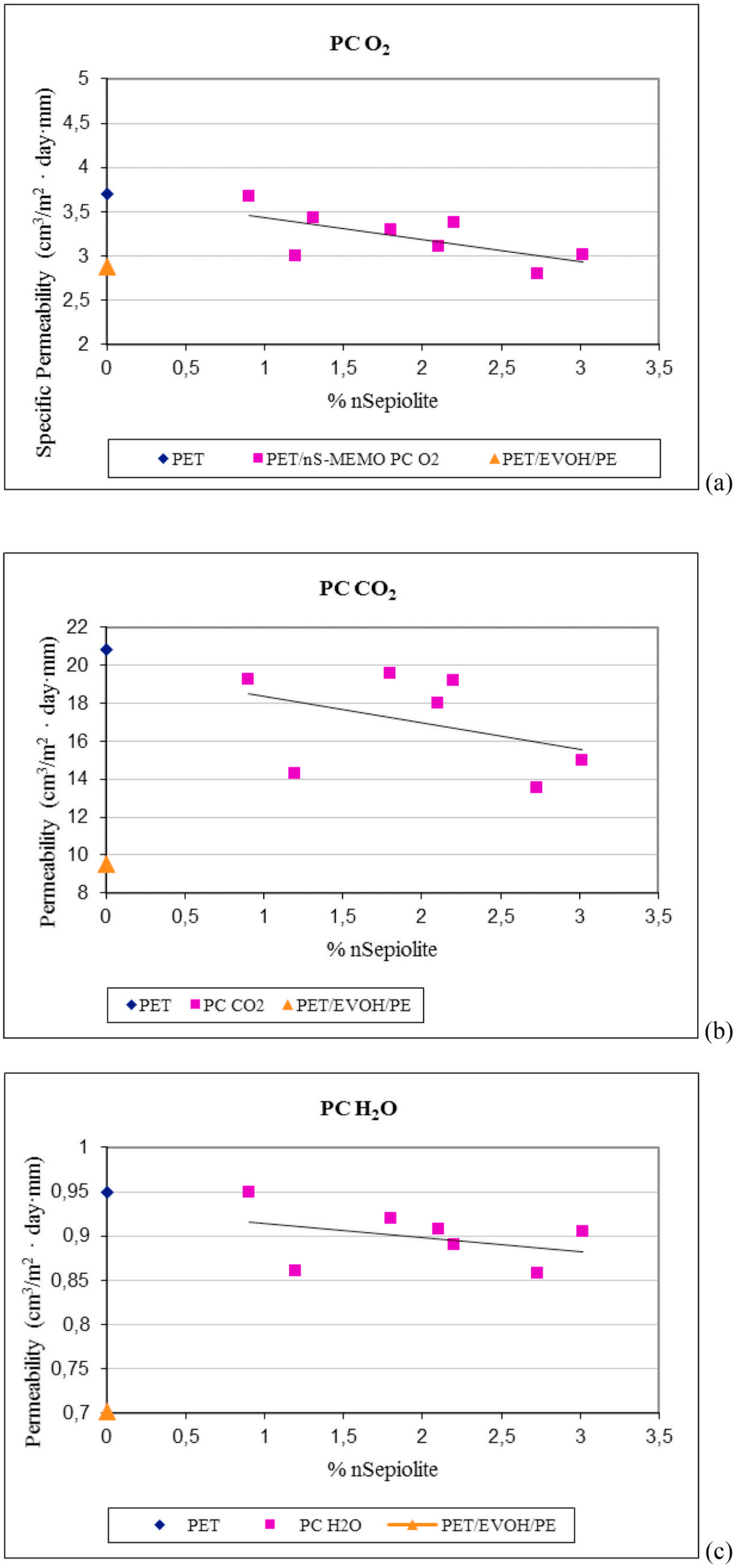

Fig. 8. Permeability versus nanosepiolite content within the nanocomposite sheets.

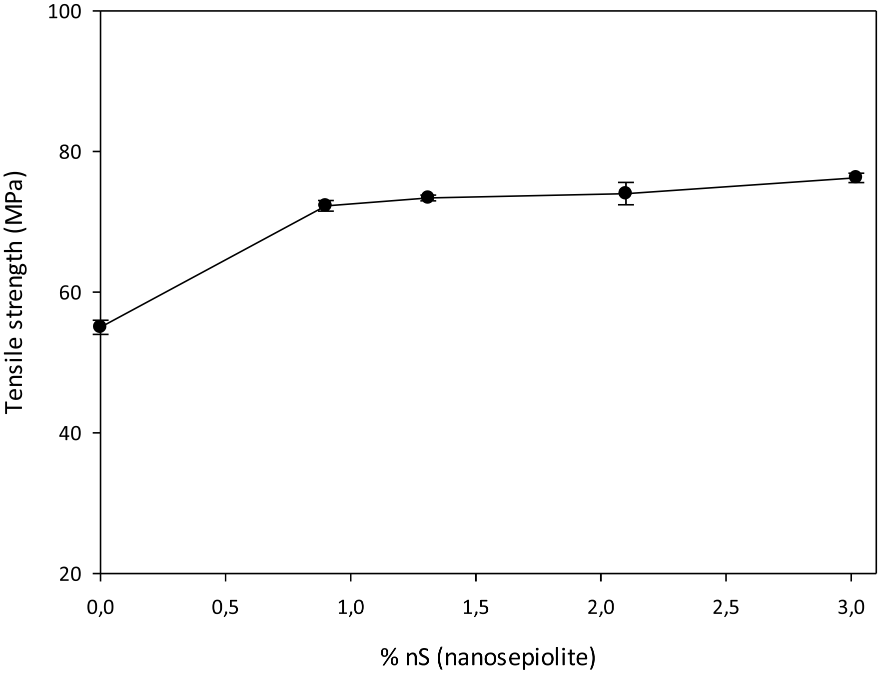

Fig. 9. Tensile strength of nanocomposite sheets as a function of sepiolite content.

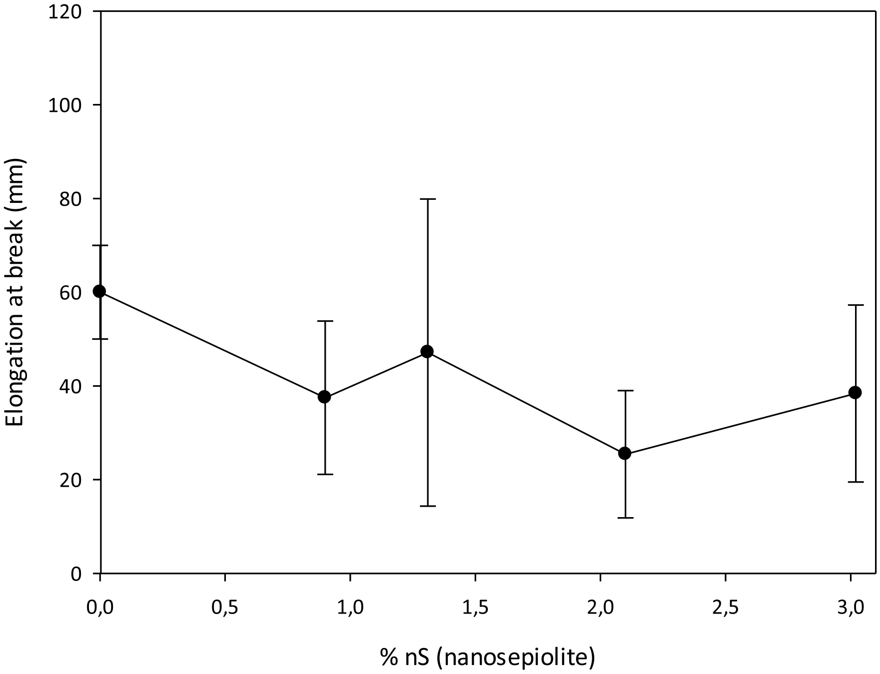

Fig. 10. Elongation at break versus sepiolite content on nanocomposites sheets.

of the nanoparticles [55]. The surface treatment of clays is a very important step in nanocomposites production, since they affect the interaction polymer-clay, the dispersion of the particles or even in the viscosity of the nanocomposites.

Once the sheets of nanocomposite have been tested, the next step is to scale up the production to industrial machines, since the objective is to produce trays with better performance for food freshness and shelf life.

3.5. Mechanical properties of nanosepiolite trays

These tests were done on equipment that has been specifically prepared for trays. Photos of the equipment are in Fig. 2a and b and Fig. 3. In both tests, results are divided by grams in order to compare all the trays produced.

Results for impact strength (illustrated in Fig. 11) are greatly influenced by the nanosepiolite concentration. We can see values between those of PET and PET-EVOH-PE when the percentage of sepiolite is lower than 2.5%. After this, the impact strength properties highly decrease. Overall, when increasing the amount of clay from 1% to 3% the impact strength is reduced up until 73%. When comparing those values with a pure PET tray, the nanocomposite trays has an impact strength 21% higher when the sepiolite content is around 1%, and 67% lower when the clay is around 3%. When increasing the nanoclay content, nanocomposites show much brittle behaviour, due to crack enlargement favoured by the nanoclay inclusions. A uniform dispersion constructs interfacial coupling between the clay and the polymer facilitating the stress transfer to the organoclay (reinforcement phase) [58, 59]. Thus, impact strength is greatly influenced by nanoclay dispersion as stated in previous works [55].

Compression tests results are done with the tray in vertical position since is, generally, the most critical force a MAP trays are going to be submitted to. Results indicate that the nanocomposite trays have more resistance to compression forces compared to the pure PET trays. Results of these tests show higher compression strength on those nanocomposites produced with lower concentration of sepiolite (Fig. 12). Also, applied load in newton per millimetre of displacement (stiffness) vs nanocomposites with different percentage of nanosepiolite and PET-EVOH-PE is shown in Fig. 13. This stiffness increases in all the samples compared to that of pure PET and it is higher than the value of PET-EVOH-PE, except for 3.02%. However, as well as in impact results, stiffness decreases when the percentage of nanosepiolite is higher than 2%, which is probably due to poorly dispersed and aligned sepiolite fibres.

4. Conclusions

From the results, it is clear that it is possible to obtain PET nanocomposite trays with improved barrier properties in an industrial process. To obtain a PET-Nanocomposite material with the best balance in properties it is necessary to control the final percentage of sepiolite. Depending on the desired properties, a percentage between 1 and 2.5% is recommended.

The permeability decreased when increasing the amount of nanosepiolite from 1% up until a point where the concentration of the nanoclay starts being too high (at 3% nanosepiolite) for a good nanocomposite processability and clay dispersion. The improvement in the permeability of PET is related to the dispersion of the nanosepiolite particles in the PET matrix, since the better the dispersion the more obstacle the gas will have to penetrate through the nanocomposite (tortuous path [49,50]). The typical acicular morphology of sepiolite can be seen in the TEM images, although some of them had been broken probably due to the nanocomposite being processed two times in different extruders. Comparing the results obtained with PET-EVOH-PE sheet, we can say that with sepiolite content of around 2%, nanocomposite permeability to O_2 is equivalent to that of PET-EVOH-PE. These barrier results could be very useful for the food packaging industry, where control of the atmosphere inside the packaging is needed for a wide range of applications. Materials used in this article comply with Royal Decree law 866/2008 and Regulation CE 975/2009 for food packaging materials, complying with global and specific migration test. The last sept to use PET/sepiolite nanocomposites in Europe would be to ask for the European Food Safety Authority (EFSA) approval.

Tensile and impact properties were measured since food packaging must resist transport, manipulation at supermarkets and it needs to arrive in perfect conditions to customers, while maintaining the product freshness and shelf life. Tensile strength is 28% higher that than or neat PET for the sample with 3% of nanosepiolite, while that value is 24% for sepiolite content of 0.9%. This means that, although there is an increase with clay content, the difference is quite small (4%). The reason for not achieving a higher tensile strength with 3% of nanosepiolite could be the poor dispersion and matrix degradation observed. These same reasons

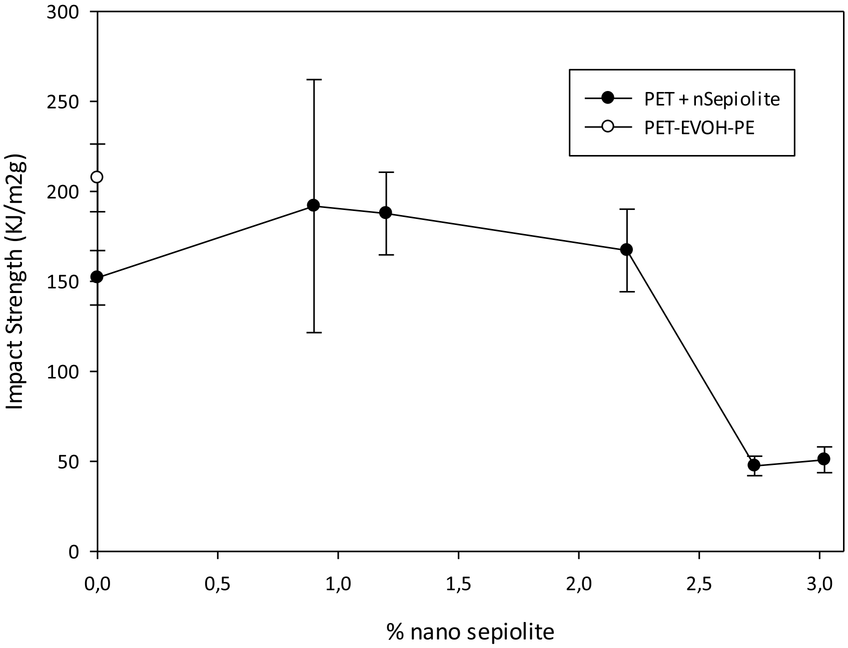

Fig. 11. Impact strength of nanocomposite trays.

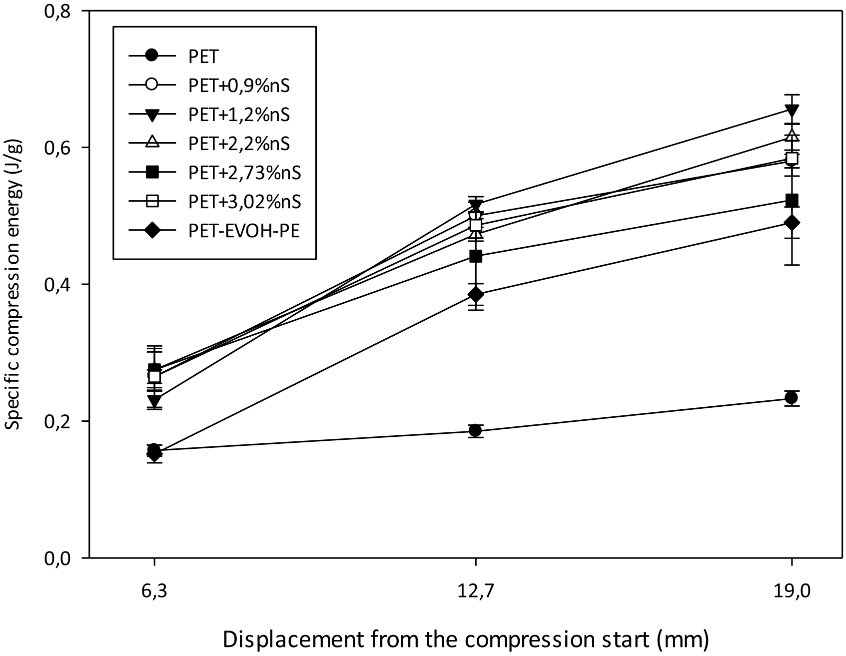

Fig. 12. Nanosepiolite/PET trays resistance to compression forces.

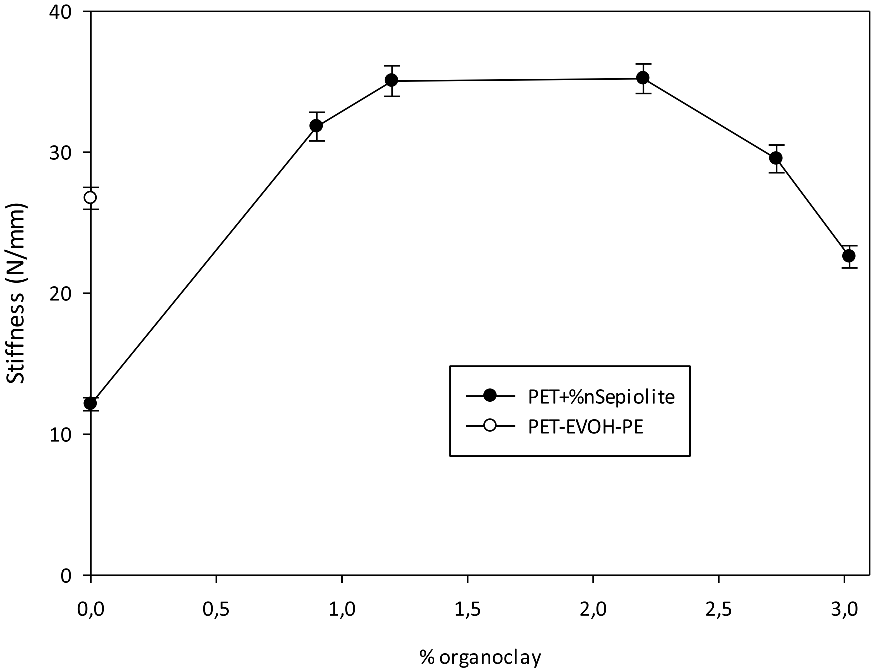

Fig. 13. Nanocomposites stiffness compared to that of pure PET and PET-EVOH-PE.

would apply to the smaller elongation at break with the maximum nanoclay loading (3%). The tests done on thermoformed trays show an impact strength 9–21% higher for those containing approximately between 1 and 2% of nanosepiolite. Also, the best results for compression forces are found in those samples with 1.2% of nanosepiolite, being up until 6 times higher than that of pure PET. Besides, all nanocomposite samples are stiffer than that of pure PET, being the stiffest ones those with sepiolite content ranging between 1 and 2%.

Declaration of competing interest

The authors declare that they have no known competing financial interests or personal relationships that could have appeared to influence the work reported in this paper.

CRediT authorship contribution statement

T. Fernández-Menéndez: Investigation, Writing - original draft. **D. García-López:** Conceptualization, Formal analysis. **A. Argüelles:** Validation, Visualization. **A. Fernández:** Methodology, Resources. **J. Viña:** Supervision. Writing - review & editing.

Acknowledgements

Authors of this paper would like to thank Klöckner Pentaplast in Pravia (former LINPAC Packaging S.A.U.), Cidaut, Ainia, Grupo Repol S. A. and Tolsa S.A. for their different collaborations in this project.

References

[1] L. Chang, C. Zhixiang, Z. Xin, M. Shirui, Nanobiomaterials in drug delivery: designing strategies and critical concepts for their potential clinical applications, in: P. Chandra, R. Prakash (Eds.), Nanobiomaterial Engineering, Springer, Singapore, 2020, pp. 253–274.

[2] R. Guazzo, Ch Gardin, G. Bellin, L. Sbricoli, L. Ferroni, F.S. Ludovichetti, A. Piatelli, I. Antoniac, E. Bressan, B. Zavan, Graphene-based nanomaterials for tissue engineering in the dental field, Nanomaterials 8–5 (2018) 349.

[3] M.I. Sierra, A. Valdés, A.F. Fernández, R. Torrecillas, M.F. Fraga, The effect of exposure to nanoparticles and nanomaterials on the mammalian epigenome, Int. J. Nanomed. 11 (2016) 6297–6306.

[4] S. Jesus, M. Schmutz, C. Som, G. Borchard, P. Wick, O. Borges, Hazard assessment of polymeric nanobiomaterials for drug delivery: what can we learn from literature so far, Front.Biotechnol. Bioeng. 7–261 (2019) 1–37.

[5] A. Roberti, A.F. Valdés, R. Torrecillas, M.F. Fraga, A.F. Fernández, Epigenetics in cancer theraphy and nanomedicine, Clin. Epigenet. (2019) 11–81.

[6] Y. Guo, X. Zuo, Y. Xue, J. Tang, M. Gouzman, Y. Fang, Y. Zhou, L. Wang, Y. Yu, M. H. Rafailovich, Engineering thermally and electrically conductive biodegradable polymer nanocomposites, Compos. B Eng. 189 (2020) 107905.

[7] J. Doh, Q. Yang, N. Raghvan, Reliability-based robust design optimization of polymer nanocomposites to enhance percolated electrical conductivity considering correlated input variables using multivariate distributions, Polymer 186 (2020) 122060.

[8] S. Fu, Z. Sun, P. Huang, Y. Li, N. Hu, Some basics aspects of polymer nanocomposites: a critical review, Nano Materials Science 1–1 (2019) 2–30.

[9] E. Thostenson, C. Li, T. Chou, Nanocomposites in context, Compos. Sci. Technol. 65 (2005) 491–516.

[10] J. Jancar, J.F. Douglas, F.W. Starr, S.K. Kumar, P. Cassagnau, A.J. Lesser, S. S. Sternstein, M.J. Buehler, Current issues in research on structure–property relationships in polymer nanocomposites, Polymer 51 (2010) 3321–3343.

[11] J.X. Li, J. Wu, X.J. Li, ChM. Chan, Thermoplastic nanocomposites, Polymer 41–18 (2000) 6935–6937.

[12] R. Krishnamoorti, R.A. Vaia, Polymer nanocomposites, J. Polym. Sci. B Polym. Phys. 45–24 (2007) 3252–3256.

[13] B.N. Jang, M. Costache, C.A. Wilkie, The relationship between thermal degradation behavior of polymer and the fire retardancy of polymer-clay nanocomposites, Polymer 46 (2005) 10678.

[14] M. Alexandre, P. Dubois, Polymer-layered silicate nanocomposites: preparation, properties and uses of a new class of materials, Mater. Sci.Eng. Rep. 28 (1–2) (2000) 1–63.

[15] E.P. Giannelis, Polymer layered silicate nanocomposites, Adv. Mater. 8 (1996) 29.

[16] A. Farahamchi, R.A. Malloy, M.J. Sobkowicz, Extreme shear processing for exfolianting organoclay in nanocomposites with incompatible polymers, Polymer 145 (2018) 117–126.

[17] S. Ray, M. Okamoto, Polymer/layered silicate nanocomposites: a review from preparation to processing progress in polymer, Science 28 (2003) 1539–1641.

[18] L. Tan, Y. He, J. Qu, Structure and properties of Polylactide/Poly(butylene succinate)/Organically Modified Montmorillonite nanocomposites with high-efficiency intercalation and exfoliation effect manufactured via volume pulsating elongation flow, Polymer 180 (2019) 121656.

[19] C. Davies, L.J. Mathias, J.W. Gilman, D.A. Schiraldi, J.R. Shields, P. Trulove, T. E. Sutto, H.C. Delong, Effects of melt-processing conditions on the quality of poly (ethylene terephthalate) montmorillonite clay nanocomposites, J. Polym. Sci. B Polym. Phys. 40 (2002) 2661–2666.

[20] B. Nagy, W.F. Bradley, The structural schema of sepiolite, Am. Mineral. 40 (1995) 885.

[21] K. Brauner, A. Preisinger, Estruktur und Enstehung des sepiolits, Mineral. Petrol. 6 (1956) 120–140.

[22] E. García-Romero, M. Suárez, Sepiolite-palygorskite: textural study and genetic considerations, Appl. Clay Sci. 86 (2013) 129–144.

[23] M. Suárez, E. García-Romero, Variability of the surface properties of sepiolite, Appl. Clay Sci. 67–68 (2012) 72–82.

[24] E. Ruiz-Hitzky, Molecular access to intracrystalline tunnels of sepiolite, J. Mater. Chem. 11 (2001) 86–91.

[25] M. Suárez, J. García-Rivas, E. García-Romero, N. Jara, Mineralogical characterisation and surface properties of sepiolite from Polatli (Turkey), Appl. Clay Sci. 131 (2016) 124–130.

[26] A. Van Meerbeek, E. Ruiz-Hitzky, Mechanism of the grafting of organosilanes on mineral surfaces, Colloid Polym. Sci. 257 (1979) 178–181.

[27] Rodov V, Shinde R, Controlled and Modified Atmospheres for Fresh and Fresh-Cut Produce 2020; Academic Press, Chapter 19.3:501-509.

[28] Bishop D, Schaefer J, Baudry R, Controlled and Modified Atmospheres for Fresh and Fresh-Cut Produce 2020; Academic Press, Chapter vol. 12:265-276.

[29] P. Suppakul, J. Miltz, K. Sonneveld, S.W. Bigger, Active packaging technologies with an emphasis on antimicrobial packaging and its applications, J. Food Sci. (2006) 62, 2.

[30] S.C. Tjong, Structural and mechanical properties of polymer nanocomposites, Mater. Sci. Eng. Rep. 53 (2006) 73–197.

[31] R. Nigmatullin, F. Gao, V. Konovalova, Polymer-layered silicate nanocomposites in the design of antimicrobial materials, J. Mater. Sci. 43–17 (2008) 5728–5733.

[32] F. Yang, Ch Mubarak, R. Keiegel, R.M. Kannan, Supercritical carbon dioxide (csCo2) dispersion of poly(ethylene terephthalate)/clay nanocomposites: structural, mechanical, thermal, and barrier properties, J. Appl. Polym. Sci. 44779 (2017) 1–11.

[33] M. Frounchi, A. Dourbash, Oxygen barrier properties of poly(ethylene terephthalate) Nanocomposite Films, Macromol. Mater. Eng. 1–294 (2009) 68–74.

[34] R. Bharadwaj, Modeling the barrier properties of polymer-layered silicate nanocomposites, Macromolecules 34 (2001) 9189–9192.

[35] L.E. Nielsen, Models for the permeability of filled polymer systems, J. Macromol. Sci. Part A. Chem. 1–5 (1967) 929–942.

[36] K. Yano, A. Usuki, A. Okada, Synthesis and properties of polyimide-clay hybrid films, J. Polym. Sci. Polym. Chem. 35 (1997) 2289–2294.

[37] A. Sánchez-Solís, A. García-Rejón, A. Martínez-Richa, F. Calderas, O. Manero, Properties of PET-PEN blends produced by extrusión and injection blow-molding, J. Polym. Eng. 25 (2005) 553–570.

[38] J.C. Matabayas Jr., S.R. Tyner, Polymer-clay nanocomposites, in: T.J. Pinnavaia, G. W. Beall (Eds.), Polymer-Clay Nanocomposites, vol. 207, John Wiley & Son, New York, 2000, p. 11.

[39] G. Gorrasi, M. Tortora, V. Vittoria, D. Kaempfer, R. Mülhaupt, Transport properties of organic vapors in nanocomposites of organophilic layered silicate and syndiotactic polypropylene, Polymer 44 (2003) 3679–3685.

[40] G. Gorrasi, M. Tortora, V. Vittoria, E. Pollet, B. Lepoittevin, M. Alexandre, P. Dubois, Vapor barrier properties of polycaprolactone montmorillonite nanocomposites: effect of clay dispersion, Polymer 44 (2003) 2271–2279.

[41] Z. Ke, B. Yongping, Improve the gas barrier property of PET film with montmorillonite by in situ interlayer polymerization, Mater. Lett. 59 (2005) 3348–3351.

[42] Y. Lin, R. Tyler, H. Sun, K. Shi, D.A. Schiraldi, Improving oxygen barrier property of biaxially oriented PET/phosphate glass composite films, Polymer 127 (2017) 236–240.

[43] ASTM E398. Standard Test Method for Water Transmission Rate of Sheet Materials Using Dynamic Relative Humidity Measurement.

[44] ASTM D3985. Standard Test Method for Oxygen Gas Transmission Rate through Plastic Film and Sheeting Using Coulometric Sensor.

[45] EN ISO 180:2001 - "Plastics. Determination of Izod impact strength".

[46] Z. Ke, B. Yongping, Improve the gas barrier property of PET film with montmorillonite by in situ interlayer pollimerization, Mater. Lett. 59 (2005) 3348–3351.

[47] Y.R. Liang, W.Q. Wang, Y.P. Wu, Y.L. Lu, H.F. Zhang, L.Q. Zhang, Preparation and properties of isobutylene-isoprene rubber (IIR)/clay nanocomposites, Polym. Test. 24 (2005) 12–17.

[48] Y.-H. Yu, J.-M. Yeh, S.-J. Liou, Ch-L. Chen, D.-J. Liaw, H.-Y. Lu, Preparation and properties of polyimide–clay nanocomposite materials for anticorrosion application, J. Appl. Polym. Sci. 92 (2003) 3573–3582.

[49] L.E. Nielsen, Models for the permeability of filled polymer systems, J. Macromol. Sci. A1 (5) (1967) 929–942.

[50] R.K. Bharadwaj, Modeling the barrier properties of polymer-layer silicate nanocomposites, Macromolecules 34 (2001) 9189–9192.

[51] E.L. Cussler, S.E. Hughes, W.J. Ward, R. Aris, Barrier membranes, J. Membr. Sci. 38 (1988) 161–174.

[52] G.H. Fredrikson, J. Bicerano, Barrier properties of oriented disk composites, J. Chem. Phys. 110 (4) (1999) 2181–2188.

[53] Q.H. Zeng, A.B. Yu, G.Q. Lu (Max), D.R. Paul, Clay-based polymer nanocomposites: research and commercial development, J. Nanosci. Nanotechnol. 5 (2005) 1574–1592.

[54] K. Majeed, M. Jawaid, Hassan, A. Abu Bakar, A. Khalil, A.A. Salema, I. Inuwa, Potential materials for food packaging from nanoclay/natural fibres filled, Mater. Des. 46 (2013) 391–410.

[55] M. Frounchi, A. Dourbash, Oxygen barrier properties of Poly(ethylene terephthalate) nanocomposite films, Macromol. Mater. Eng. 294 (2009) 68–74.

[56] S.Y. Fu, B. Lauke, Effects of fiber length and fiber orientation distributions on the tensile strength of short-fiber-reinforced polymers, Compos. Sci. Technol. 56 (1996) 1179–1190.

[57] A. Sánchez-Solis, I. Romero-Ibarra, M.R. Estrada, F. Calderas, O. Manero, Mechanical and rheological studies on polyethylene terephthalate-montmorillonite nanocomposites, Polym. Eng. Sci. 44 (2004) 1094–1102.

[58] F. Hussain, M. Hojjati, M. Okamoto, R.E. Gorga, Review article: polymer-matrix nanocomposites, processing, manufacturing, and application: an overview, J. Compos. Mater. 40 (2006) 1511–1575.

[59] G. Lagaly, Introduction: from clay mineral-polymer interactions to clay mineral -polymer nanocomposites, Appl. Clay Sci. 15 (1999) 1–9.